Proc. of Kofu Symposium, NRO Report No. 360, July, 1994

OVRO AND NRO OBSERVATIONS OF THE SOLAR FLARE ON 1993 JUNE 3

D. E. Gary [1], S. Enome [2], M. Bruner [3]

[1] *Solar Astronomy 264-33, Caltech, Pasadena CA 91125, U.S.A.*
[2] *Nobeyama Radio Observatory, Minamisaku, Nagano, 384-13, Japan*
[3] *Lockheed Palo Alto Research Laboratory, ORG 91-30, Bldg 255, 3251 St., Palo Alto, CA 94304, U.S.A.*

Abstract

A flare that began on 1993 June 3 was observed jointly by the Owens Valley Radio Observatory (OVRO) Solar Array and the Nobeyama Radio Observatory (NRO) Radioheliograph. We present preliminary results from these observations, along with soft X-ray data from the Yohkoh SXT and GOES. The burst had a gradual time profile in the 17 GHz NRO data, except for a pair of unusual spikes in the decay phase. However, the OVRO data show that the burst was impulsize, comprising several peaks at progressively higher frequencies. We suggest that the gradual 17 GHz emission is thermal, and discuss the relationship of the thermal emission to the impulsive emission.

1. Introduction

A unique aspect of the NRO Radioheliograph (Nakajima et al. 1994) is its ability to give high spatial resolution images of extended, low surface brightness radio sources in the optically thin part of the radio spectrum. The 1993 June 03 flare was dominated by such low-brightness emission at 17 GHz while at lower frequencies, as seen with the OVRO Solar Array, the burst showed more typical impulsive characteristics. These observations allow us to investigate the relationship between these two emission components.

Joint observations between NRO and OVRO are quite rare, because of the short, approximately 1 h overlap in observing periods that occurs only during the summer months. With our entry into the current solar minimum, joint burst observations may remain rare for some time. Joint observations are desirable, however, because of the complementarity of the two instruments. The OVRO spectral coverage is useful to place the NRO emission at 17 GHz into context. It helps to determine the emission mechanism responsible for the 17 GHz sources. At the same time, the OVRO imaging capability is restricted to the brightest sources and has little sensitivity to extended emission. Here the high quality NRO images play an important role in understanding the OVRO emission. Together, the two instruments give a more complete view than either alone.

In the present event, additional information in soft X-rays from the Yohkoh SXT and from GOES has also proved to be important. Combining these data, we find that the bulk of the 17 GHz emission in this burst is thermal, while the lower frequency emission is dominated by impulsively accelerated nonthermal electrons. In this paper we discuss the relationship between these components.

2. Observations

The flare occurred in region complex NOAA 7514-7515, at 15N 50W, and reached GOES class M1.0. The maximum OVRO flux was 45 SFU, which was reached at 6.6 GHz at 2322 UT.

Figure 1*a* shows an overview of the flare as observed by OVRO in the form of a dynamic spectrum in total flux and Figure 1*b* compares the light curves from OVRO, GOES, and NRO to the same time scale. The NRO curve shows the maximum T_b in each of the 103 maps used in this study, made every 30 s except during the spikes, when the maps were made every 1 s. A light curve (not shown) of the NRO 17 GHz integrated flux, obtained by summing the maps, was similar to the T_b curve. The light curves in Figure 1*b* show that except for the pair of spikes near 2334 UT, the NRO curve shows a gradual temporal evolution almost identical to the soft X-ray time profile from GOES. In the OVRO time profile at 7.4 GHz, however, impulsive behavior is evident early in the burst. In the dynamic spectrum in Fig. 1*a*, the spectral range of the impulsive emission is seen to move to higher frequencies in later peaks, and extends to 17 GHz in the pair of spikes near 2334 UT.

The spatial distribution of these emission components are shown in Figure 2. The four times shown are 2322 UT—the peak of the impulsive burst seen at OVRO; 2329 UT—the peak of the first gradual component seen with GOES and NRO; 2335 UT—the peak of the second spike seen with OVRO and NRO; and 2338 UT—early in the gradual phase after the spikes. These times are denoted by arrows along the time axis of Fig. 1. Although Yohkoh unfortunately missed the beginning of the event, the subsequent development shows that the pair of radio spikes near 2334 UT (third panel in Fig. 2) mark the brightening of an arcade of small loops that were not visible before 2334 UT. This arcade continued to grow eastward throughout the rest of the event. The OVRO source is double during the impulsive peaks (first and third panels of Fig. 2), but appears to be single between the peaks.

Summarizing the radio emission characteristics, we find the following: (i) Brightness temperature of the OVRO impulsive sources, derived from the 6-9 GHz frequency synthesis maps, was 1.4×10^7 K at 2322 UT, and 9×10^6 K at 2335 UT, but between the impulsive peaks it reached only $3\text{-}4 \times 10^6$ K. (ii) The brightness temperature seen at 17 GHz from NRO was more than an order of magnitude lower, ranging from $1\text{-}3 \times 10^5$ K during the gradual phase to 4.7×10^5 K during the spikes. (iii) The circular polarization was very low throughout the burst, increasing from 2 to 6% left-hand (LH) during the gradual emission and changing sign to 1% right-hand (RH) during the spikes. The impulsive emission seen with OVRO was slightly ($< 10\%$) RH polarized.

3. Discussion

The low brightness temperature ($< 10^6$ K) of the gradual component at 17 GHz indicates that the emission is optically thin. This, combined with the low circular polarization ($< 10\%$) suggests that the 17 GHz emission is due to free-free emission. The agreement in light curves for NRO and GOES in Fig. 1 offers strong support for this suggestion, as does

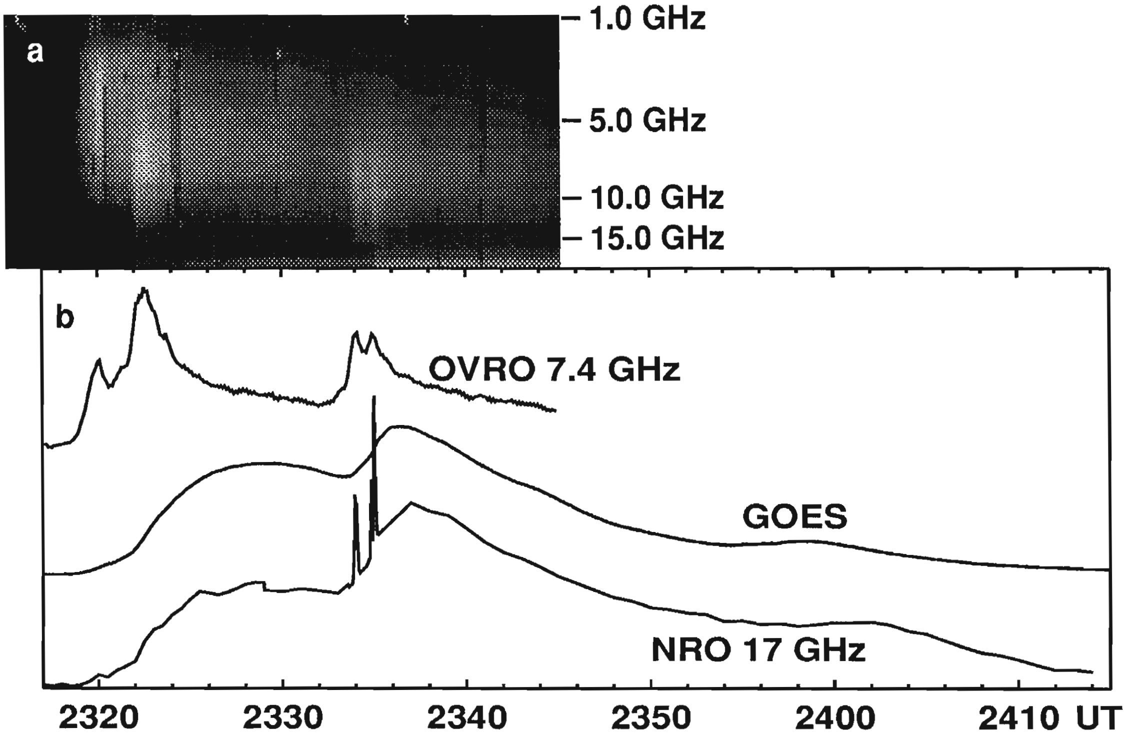

Fig. 1. Overview of the flare. (*a*) Dynamic spectrum from OVRO total power data, showing several impulsive peaks occurring at progressively higher frequencies. (*b*) OVRO, GOES, and NRO light curves to the same time scale as in *a* (arbitrary linear vertical scale). The arrows mark the times of the images shown in Fig. 2.

the detailed correspondence between the Yohkoh and NRO images in the second and fourth panels of Fig. 2.

In contrast, the OVRO emission below about 10 GHz is dominated by a higher brightness temperature (higher energy), impulsive component of a quite different spatial distribution. Although the brightness temperature of the impulsive component measured by OVRO is within the range detectable by GOES (Thomas et al. 1985) there is no sign of this component in the GOES light curve of Fig. 1, implying that the OVRO emission is due to a relatively small number of nonthermal electrons. There is insufficient information available to determine the magnetic field structure responsible for the difference in spatial distributions of the impulsive and gradual components, but clearly some magnetic loops must exist that connect the two OVRO sources but are not visible in either Yohkoh or NRO images.

Recently, a paper by Nishio et al. (1994) has discussed the evolution of thermal and nonthermal radio sources observed with the Nobeyama Radioheliograph. The radio sources were interpreted in terms of a single loop with the nonthermal source at one of the footpoints and two thermal sources located near the loop top, supplied by chromospheric evaporation. A similar explanation will serve for this event, with the exception that a second loop system must be involved to account for the OVRO double source structure during the impulsive peaks. An explanation for the present burst that is consistent with our observations is that interaction of magnetic loop systems initiated an explosive energy release into more than one system of loops. The energy release was initially impulsive, accounting for the OVRO impulsive component, but quickly evolved into primarily thermal emission in small, relatively dense loops, giving rise to the gradual component, similar to the case discussed by Nishio et al. (1994). However,

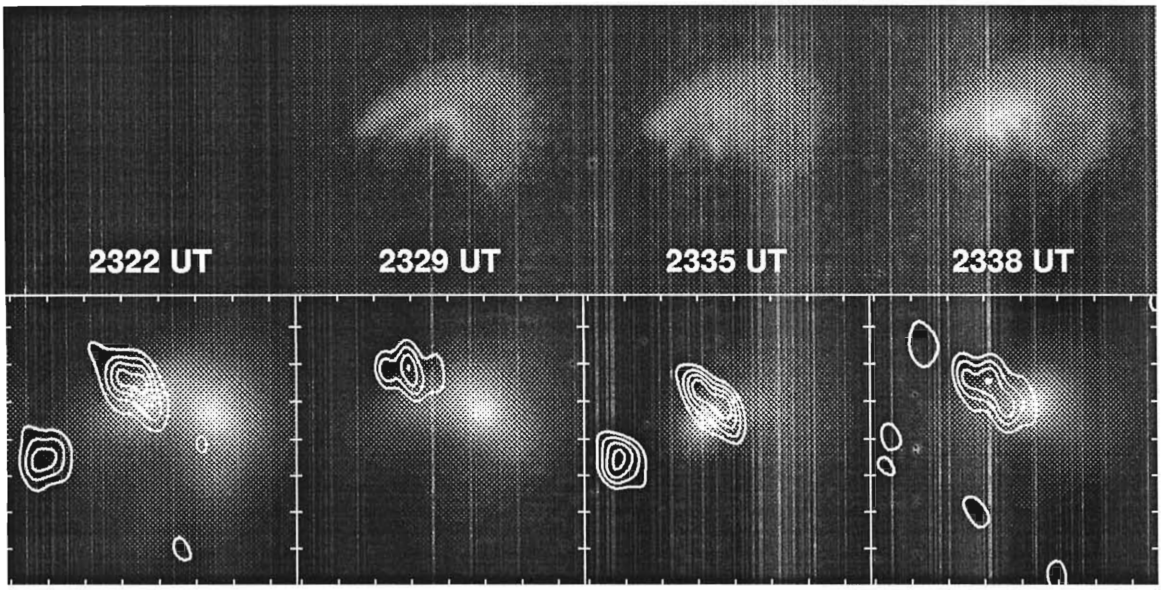

Fig. 2. Spatial distribution of the emission shown in Fig. 1. Each row of four images corresponds to the times shown. The top row gives the Yohkoh Be filter images while the bottom row shows the corresponding NRO 17 GHz maps (grayscale) and the 6-9 GHz OVRO maps (contours). The tick marks on the bottom panel axes are 20″ apart. Solar north is up, and west is to the right.

additionally a relatively small fraction of these nonthermal electrons were accelerated within the larger, less dense loop that connects the two OVRO sources.

In recent studies with OVRO data we have seen important spatial differences between some microwave and soft X-ray sources (Lim et al. 1994, Wang et al. 1994). We have attributed the secondary microwave sources to emission by a small number of electrons in regions of strong magnetic field, where no appreciable soft X-rays are emitted. Differences in source structure between microwaves and X-rays, and even from one microwave frequency to the next, appear to be quite common. The differences go to show that while individual emission bands show great detail in the physical parameters to which they are sensitive, they can and generally do miss other parameters that are just as important to understanding the flare. Such observations as we have described also underscore the importance of both spatially and spectrally resolved observations. Joint observations between OVRO and NRO will continue to be important for these reasons.

Acknowledgements: The OVRO Solar Array is supported by NSF grants ATM-9311416 and AST-9314292 to Caltech. DG gratefully acknowledges the financial assitance from the organizers of the Kofu Symposium that allowed his attendance at the meeting.

References

1. Lim, J., Gary, D.E., Hurford, G.J., and Lemen, J.R. 1994, *Ap. J.* in press.
2. Nakajima, H. and 16 others, 1994, *Proc IEEE* in press.
3. Nishio, M., and 16 others, 1994, *PASJ* **46**, L11.
4. Thomas, R.J., Starr, R., and Crannell, C.J. 1985, *Solar Phys.* **95**, 323.
5. Wang, H., Gary, D.E., Zirin, H., Nitta, N., and Schwartz, R.A. 1994, in preparation.